Journal of Nuclear Materials 532 (2020) 152049

Contents lists available at ScienceDirect

Journal of Nuclear Materials

journal homepage: www.elsevier.com/locate/jnucmat

A simple and effective separation of UO_2 and Ln_2O_3 assisted by NH_4Cl in LiCl–KCl eutectic

Yi-Chuan Liu [a, b], Ya-Lan Liu [a, **], Yuan Zhao [c], Zhe Liu [c], Tong Zhou [c], Qing Zou [c], Xian Zeng [c], Yu-Ke Zhong [a], Mei Li [b], Zhong-xuan Sun [b], Wei-Qun Shi [a, *]

[a] *Laboratory of Nuclear Energy Chemistry, Institute of High Energy Physics, Chinese Academy of Sciences, Beijing, 100049, China*
[b] *Key Laboratory of Superlight Materials and Surface Technology, Ministry of Education, College of Material Science and Chemical Engineering, Harbin Engineering University, Harbin, 150001, China*
[c] *Reactor Engineering and Safety Research Center, China Nuclear Power Technology Research Institute Co., Ltd, China General Nuclear Power Corporation, Shenzhen, 518000, China*

GRAPHICAL ABSTRACT

In this work, a new method with the assistance of NH_4Cl to directly separate UO_2 and Ln_2O_3 in Ar atmosphere that does not require an electrochemical process is reported. The separation is achieved by dissolving Ln_2O_3 with NH_4Cl into the LiCl–KCl molten salt, while UO_2 is not reacted with NH_4Cl and still exists in a solid form.

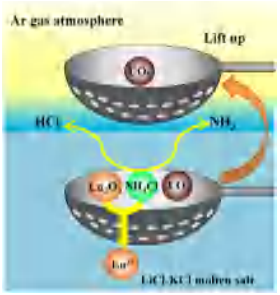

ARTICLE INFO

Article history:
Received 28 November 2019
Received in revised form
30 January 2020
Accepted 9 February 2020
Available online 13 February 2020

Keywords:
Separation
NH_4Cl
UO_2 and La_2O_3
LiCl–KCl eutectic salt

ABSTRACT

For UO_2-based spent fuel, it is usually electrochemically reduced and then refined in molten salt with respect to the so-called pyrochemical reprocessing approach. In this work, we report a new method with the assistance of NH_4Cl to directly achieve convenient separation of UO_2 over La_2O_3 in Ar atmosphere which does not require an electrochemical process. According to the results from both powder and pellet samples, the separation is achieved by dissolving La_2O_3 into the LiCl–KCl molten salt with NH_4Cl, whilst UO_2 cannot be dissolved and remains in solid form. It was found that the dissolution kinetics of La_2O_3 in the powder sample was fast and its removal efficiency in the mixture of La_2O_3 and UO_2 was high, but a specific amount of UO_2 was also dissolved, which lead to a low recovery efficiency of UO_2. In contrast, when the pellet samples after sintering at 1473 K were used, the recovery efficiency of UO_2 can be increased. Nevertheless, the dissolution kinetics of La_2O_3 was correspondingly reduced, and more NH_4Cl was required to complete the dissolution reaction. By improving and optimizing the experimental conditions, the UO_2 recovery efficiency of 92.0% can be achieved, while the removal efficiency of La_2O_3

* Corresponding author.
** Corresponding author.
E-mail addresses: liuyalan@ihep.ac.cn (Y.-L. Liu), shiwq@ihep.ac.cn (W.-Q. Shi).

https://doi.org/10.1016/j.jnucmat.2020.152049

was 94.4%. More importantly, this novel separation method may be also useful for the separation of UO_2 over mixed lanthanide oxides.

1. Introduction

It is well-known that uranium dioxide (UO_2) is the most important ceramic component of nuclear fuel [1], and therefore is also a main product in the spent fuels [2]. Up to now, a lot of research efforts have been made on the pyrochemical process of UO_2-based spent fuel for the advanced fuel cycle of Generation IV reactors [3–5]. In general, UO_2-based spent fuel is reduced to metal U in LiCl–Li_2O melt [6–11], and then purified by the following electrorefining process to remove lanthanide (Ln) fission products (FPs) [3,5,12]. However, since the deposition potential of the Ln is more negative than that of U [13–17], the separation of U over Ln can be achieved by selectively depositing U on the cathode [1,8,18–20]. Actually, the proportion of Ln-FPs in the spent fuel is low, with the total percentage of about 1% [21–25]. Thus, recovering a large amount of U and removing a small amount of Ln-FPs by electrorefining strategy is somewhat uneconomical from perspective of energy consumption. In recent years, some researchers have been seeking for more convenient and economic methods to strip small amounts of Ln-FPs out of spent fuel rather than directly electrolyzing a large amount of U. For example, the separation of Nd_2O_3 and UO_2 in ionic liquid [Hbet][Tf_2N] in a simple manner was studied based on the solubility difference of Nd_2O_3 and UO_2 in this media [22].

In our previous work, we found that the dissolution of lanthanide oxides (Ln_2O_3) in LiCl–KCl molten salt can be achieved readily by using ammonium chloride [23], and the dissolution of Ln_2O_3 is much easier than that of UO_2. Therefore, if the difference of solubility between UO_2 and Ln_2O_3 is properly utilized, separation of UO_2 from Ln_2O_3 with assistance of ammonium chloride should be possible. According to the thermodynamic analyses, we believe that UO_2 will not react with NH_4Cl in an inert atmosphere at 723 K [23]. Therefore, a new approach for separating UO_2 over Ln_2O_3 is proposed in this work by dissolving Ln_2O_3 in molten salt under argon atmosphere assisted by NH_4Cl. In this way, the Ln_2O_3 is converted into corresponding chlorides and dissolved in the LiCl–KCl molten salt, whilst UO_2 is insoluble and can be recovered directly in remnants. It may generate a new opportunity to significantly simplify the so-called pyrochemical process by overriding the use of electrochemical method and may provide a new design idea for recovering actinides over FPs in molten salt media.

2. Experiment

2.1. Materials and equipment

Lithium chloride, potassium chloride, and ammonium chloride (anhydrous, AR grade, Aladdin Reagent (Shanghai) Co., Ltd) were used in the study. UO_2 was purchased from CNNC North nuclear fuel element Co., Ltd. La_2O_3, Sm_2O_3, and Nd_2O_3 of >99.99% purity were purchased from Baotou Rare-earth Co., Ltd. Mo basket and crucible (as shown in Fig. 1) were used to load the mixture of NH_4Cl, UO_2 and Ln_2O_3. The molybdenum crucible was 15 mm in diameter, 50 mm in height, and with several small holes of 1 mm diameter on its bottom. The Mo basket is compiled by dense Mo mesh (record as 1#), which was purchased from Anping ChenYi Wire Mesh Products Co., Ltd and the filter aperture of the mesh is 40 μm. When the separation experiments were carried out with molybdenum crucibles, a layer of 2# Mo mesh (filter aperture 87 μm, 200 mesh) was placed on the bottom of the crucible for sample 1 and two layers of molybdenum mesh (one layer 1#, one layer 2#) were placed for other samples, to prevent UO_2 powder from leaking from the small holes.

The tube type resistance-heated furnace (FNS-Beijing electric Furnace Co., Ltd) is used for sintering pellet samples. Inductively coupled plasma atomic emission spectrometer (ICP-AES, Horiba, JY, 2000-2) were used to monitor the extent of the separation process. Agilent Cary 5000 UV-Vis-NIR spectrometer was used for in-suit electron absorption spectrum measurements. The obtained products were analyzed by XRD (Bruker D8).

2.2. Preparation of LiCl–KCl eutectic, oxide powders and pellets mixture

A mixture of LiCl–KCl (44.8: 55.2 wt% mixed) was placed in the graphite corundum crucible and then dried in a vacuum drying box at 373 K more than 72 h. After that, the graphite crucible was removed to the electric furnace in the glove box heating at 773 K for 48 h (the heating rate is 10 K/min), and then naturally cooled down to room temperature.

The UO_2 and Ln_2O_3 powder (total mass about 0.50 g) with different mass ratio of Ln_2O_3 was mixed by a vortex mixer for 10 min. The pellets were prepared as follows [26,27]: first of all, Ln_2O_3 and UO_2 powder with different mass ratio was ball-milled with PVB (1 wt%) for 10 min. Then about 0.5 g of mixture was pressed into cylindrical pellets (10 mm in diameter, 0.8 mm in thickness) in the hydraulic press under 10 MPa. Then the pellets were subjected to sintering at 1473 K for 10 h under 4% Argon-hydrogen mixed atmosphere in a tube type resistance-heated furnace.

2.3. Separation methods

The schematic illustration for the separation of powder mixture in Mo crucible is shown in Fig. 2, similar separation steps were conducted for both powder samples and pellet samples. First of all, the prepared LiCl–KCl quenched salt was placed in the cylindrical corundum crucible (60 mm in diameter, 120 mm in height) and heated to 723 K in the electric furnace placed in a glove box with a heating rate of 5 K/min. Then the prepared Ln_2O_3-UO_2 samples were loaded in the Mo crucible or Mo basket, and then covered with NH_4Cl powder. After that, the Mo crucible or Mo basket with the mixed powder was placed into LiCl–KCl molten salt at 723 K for further separation experiments. During the separation process, a

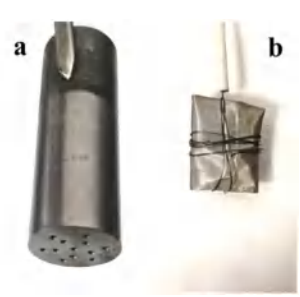

Fig. 1. (a) The Mo crucible and (b) Mo basket as the container to load the powders or pellets.

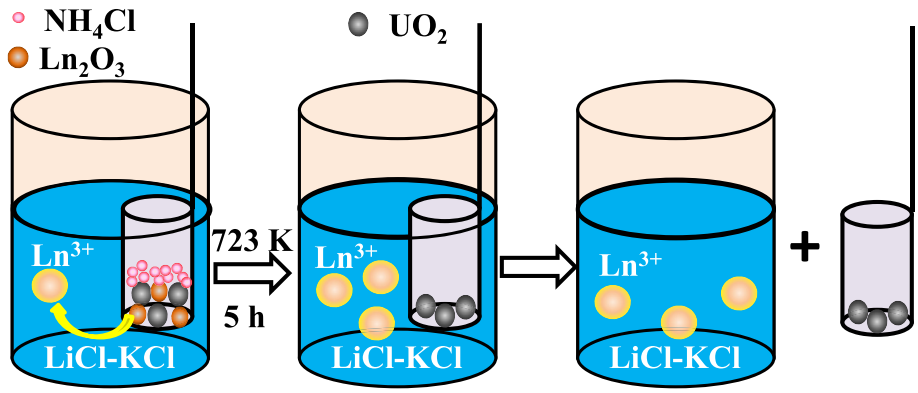

Fig. 2. Schematic illustration of UO_2 separation over Ln_2O_3 in the Mo crucible.

cool corundum tube was regularly inserted into the molten salt and instantly removed out, thus some of the salt was adhered onto the corundum tube, and these quenched salts were then stripped from the corundum tube and collected for subsequent analysis [23]. The salt samples were collected at 30, 60, 120, 180 and 300 min, respectively. The collected salts were then dissolved in ultrapure water, filtered with a syringe filter (MCE, 0.22 μm), and used for ICP-AES analysis.

When the reaction of Ln_2O_3 is completed, the Mo crucible or Mo basket was taken out directly from molten salt to recover UO_2. The recovered UO_2 was washed with ultrapure water, vacuum filtered and then dried in a vacuum oven for further weighting. Then a portion of each dried sample was dissolved in concentrated nitric acid, and then diluted with ultrapure water for ICP-AES measurements. The residual amount of Ln_2O_3 in the recovered UO_2 products was analyzed to calculate the removal efficiency of Ln_2O_3. All separation experiments were performed in a glove box, in which the level of oxygen and water was strictly controlled to be less than 2.0 ppm.

3. Results and discussion

3.1. Thermodynamic evaluation of the feasibility for the separation of UO_2 and Ln_2O_3

As reported in our previous study [23], the reactions related to the dissolution of UO_2 and Ln_2O_3 with NH_4Cl in the LiCl–KCl molten salt are as follows:

$$UO_2(s) + 4NH_4Cl(s) = UCl_4(l) + 4NH_3(g) + 2H_2O(g) \quad (1)$$

$$2UO_2(s) + O_2(g) + 4NH_4Cl(s) = 2UO_2Cl_2(l) + 4NH_3(g) + 2H_2O(g) \quad (2)$$

$$Ln_2O_3(s) + 6NH_4Cl(s) = 2LnCl_3(l) + 6NH_3(g) + 3H_2O(g) \quad (3)$$

Fig. 3 shows the standard Gibbs free energy changes ($\Delta^{\theta}G_m$, obtained by software HSC chemistry 6.0) of reactions (1), (2) and (3) as a function of temperature. It can be found that for all the three reactions, the $\Delta^{\theta}G_m$ decreases with the increase of temperature, indicating that a higher temperature will promote all the three reactions. Reaction (2) corresponds to the dissolution of UO_2 in air, and the $\Delta^{\theta}G_m$ value of this reaction is about 0 kJ mol^{-1} at 437 K. When the temperature is higher than 437 K, the reaction proceeds spontaneously, which has been confirmed in our previous study [23]. Similarly, reaction (3) corresponds to the dissolution of Ln_2O_3, which is also spontaneous above 437 K. As the melting point of LiCl–KCl eutectic is about 625 K, reactions (2) and (3) may occur

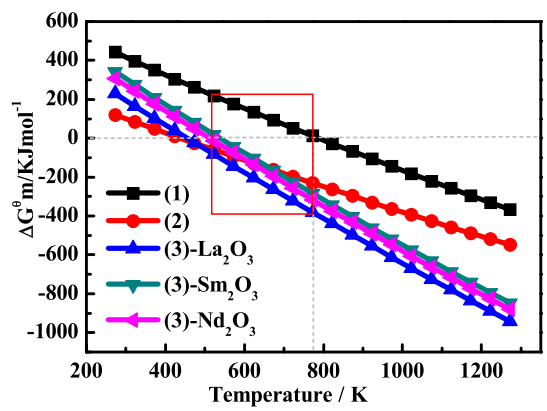

Fig. 3. The relationship between $\Delta^{\theta}G_m$ and temperature of reaction (1), (2), and (3).

simultaneously in this molten salt. Therefore, it is impossible to separate UO_2 and Ln_2O_3 in an air atmosphere by using NH_4Cl.

Conversely, the $\Delta^{\theta}G_m$ value of reaction (1) corresponding to the dissolution of UO_2 in an inert gas atmosphere is > 0 when the temperature is below 789 K. Therefore, UO_2 is theoretically insoluble in LiCl–KCl molten salt below 789 K, which allows the separation of UO_2 over Ln_2O_3 based on their difference in solubility, as envisioned in Fig. 2. In order to achieve a faster dissolution kinetics of Ln_2O_3, a higher temperature of 723 K was selected over the feasible temperature range. At 723 K, the $\Delta^{\theta}G_m$ value of reaction (1) is 52.59 kJ mol^{-1}, thereby ensuring that UO_2 does not react with NH_4Cl to form UCl_4. In contrast, the $\Delta^{\theta}G_m$ of reaction (3) for La_2O_3, Sm_2O_3 and Nd_2O_3, respectively, is −322.15, −224.77 and −256.04 kJ mol^{-1}, respectively, which means it is possible to dissolve La_2O_3, Sm_2O_3 and Nd_2O_3 easily by forming corresponding chlorides.

3.2. Separation of UO_2 and La_2O_3 powder

Fig. 4 shows the dissolution of powder samples in LiCl–KCl molten salt, and the specific details of experiment conditions are shown in Table 1. The dissolution efficiency here is obtained by measuring the concentration of La^{3+} ions in molten salt by ICP-AES. The dissolution efficiency of Ln_2O_3 (or UO_2) is determined by the following formula:

$$\eta_{\text{dissolution}} = \frac{C_M \times m_0}{\alpha \times m_1} \times 100\% \quad (4)$$

where C_M is the concentration of M (M = U or Ln) ions in molten salt, m_0 corresponds the mass of LiCl–KCl salt, m_1 represents the

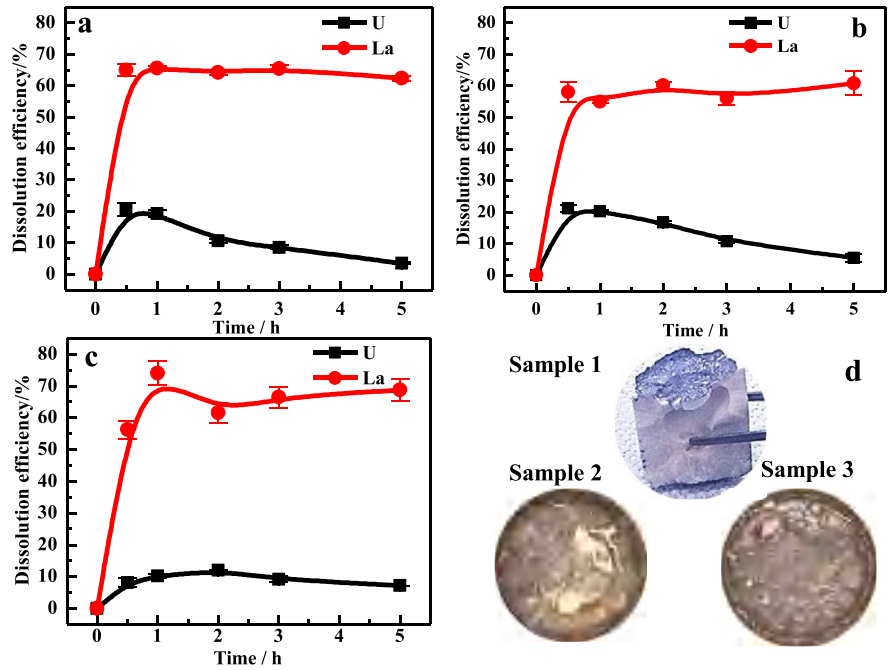

Fig. 4. Dissolution efficiency of UO_2 and La_2O_3 for powder samples at 723 K: (a) sample 1, (b) sample 2, and (c) sample 3; and (d) the quenched salts after separation.

Table 1
The experimental conditions and separation results of UO_2 and La_2O_3 at 723 K.

Sample No.	Sample form	La_2O_3 content /wt%	m (UO_2+ La_2O_3)/g	m_0 (LiCl−KCl)/g	m (NH_4Cl)/g	C_U in melt /wt%	C_{La} in melt /wt%	m_2 (recovery sample) /g	m_3 (residual La_2O_3)/g	$\eta_{recovery}$ (UO_2)	η_{remove} (La_2O_3)
1	powder	1.3	0.503	80	2.0	0.0186	0.0042	–	–	–	–
2	powder	1.1	0.499	100	2.0	0.0243	0.0028	0.077	0.0000	15.4%	100%
3	powder	1.1	0.498	250	2.0	0.0124	0.0013	0.327	0.0000	65.6%	100%
4	pellet	1.0	0.480	40	2.0	0.0000	0.0015	0.455	0.0018	95.4%	63.1%
5	pellet	5.4	0.476	40	2.0	0.0023	0.0210	0.451	0.0046	99.2%	82.0%
6	pellet	10.8	0.470	40	2.0	0.0028	0.0467	0.364	0.0218	81.6%	57.0%
7	pellet	1.0	0.476	76	3.5	0.0019	0.0018	0.434	0.0003	92.0%	94.4%

mass of Ln_2O_3 (or UO_2), and α designates the mass fraction of M in its corresponding oxide.

As shown in Fig. 4a–c, the dissolution efficiency of La_2O_3 in samples 1, 2 and 3 were 64.9 ± 2%, 58.0 ± 3% and 56.3 ± 5%, respectively, for the dissolution time of 0.5 h. When the reaction proceeded to 5 h, the efficiency was 62.4 ± 1%, 60.9 ± 3%, 68.8 ± 4%, respectively. It is clear that the dissolution efficiency of La_2O_3 does not change much between dissolution time of 0.5 and 5 h, which indicates that the dissolution kinetics of La_2O_3 is fast, and the dissolution reaction can be completed in almost 0.5 h. Therefore, the dissolution time of 5 h should be absolutely sufficient for La_2O_3 transformation.

It is envisaged that when La_2O_3 is completely dissolved, and the Mo crucible or basket loaded with UO_2 is lifted from molten salt, the separation of UO_2 and La_2O_3 should be achieved. Nevertheless, for sample 1, when we lifted the crucible (a layer of 2# molybdenum mesh was placed in crucible bottom) from molten salt, it was found that almost no UO_2 powder was collected in it. As shown in Fig. 4d, all of UO_2 powder leaked out from the crucible through the molybdenum mesh and floated on the surface of molten salt, which should be related with the tiny size of UO_2 powder particle. In addition, it was found that UO_2 was partially dissolved in molten salt with the dissolution efficiency of 21 ± 2% and 3 ± 0.3% at 0.5 h and 5 h, respectively. In order to determine the dissolution of UO_2,

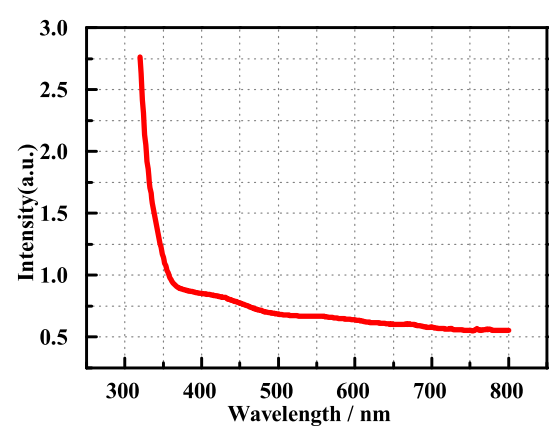

Fig. 5. In-situ UV–Vis spectrum of the molten salt for operating sample 1 at 723 K.

the salt of sample 1 was analyzed by in-situ UV–Vis measurement and the result was shown in Fig. 5. The absorption spectrum has a small absorption band at around 430 nm, and a strong absorption band below 360 nm. The absorption observed here was very different from that of U(IV) species which have a conspicuous band

at 600–700 nm [28–30], but was similar to that of UO_2^{2+} dissolved in the LiCl–RbCl molten salt or LiCl–KCl molten salt at 673 K [31,32]. Thus, it is reasonable to believe that UO_2 is dissolved and converted into uranyl species in molten salt. The formation of uranyl is due to the small amount of oxygen contained in the melt or the glove box. UO_2 is oxidized to a high-valent oxide (UO_3 or U_3O_8) at high temperature and then reacts with NH_4Cl to form UO_2Cl_2. This process can be expressed in reaction (2) that has been reported in previous work [23]. Therefore, although the concentration of O_2 in the glove box is strictly controlled, the UO_2 powder can be still partially oxidized and dissolved due to the trace amount of O_2 in the glove box.

However, when the UO_2 powder was pressed into a pellet and immersed into the molten salt, almost no dissolution of UO_2 was observed. The possible explanation is that the oxidation and dissolution of UO_2 can only occur on the surface of LiCl–KCl molten salt due to the presence of trace amount of oxygen in glove box, and the UO_2 pellet sample in molten salt is less likely to be exposed to trace amount of oxygen than that of UO_2 powder sample. In addition, it was found that for the samples 1–3, the measured dissolution efficiency of UO_2 decreased as the dissolution time increased. This may be correlated with the sampling process which was conducted on the upper layer of molten salt. It should be noted that soluble UO_2^{2+} ions are formed on the surface of molten salt, and the concentration of soluble U(VI) in the upper layer melt should be higher in the initial stage of the dissolution process due to the limited diffusion coefficient of U(VI) in molten salt. Subsequently, the soluble UO_2^{2+} ions continuously diffused to the bottom of molten salt, and the concentration of U(VI) was ultimately the same in the total molten salt system.

The leakage of UO_2 powder from the crucible was unfavorable for the recovery of UO_2. To decrease this leakage, for the separation experiment of sample 2, two layers of molybdenum mesh (layer 1# and layer 2#) were placed on the bottom of Mo crucible. As shown in Table 1, 15.4% UO_2 was recovered, the recovery efficiency was still too low, and most of UO_2 was still floating on the surface of molten salt (Fig. 4d). The recovery efficiency of UO_2 was determined by the equation (5) as follows:

$$\eta_{recovery} = \frac{m_2 - m_3}{m_4} \times 100\% \tag{5}$$

Where m_2 is the mass of recovered sample, m_3 corresponds to the mass of residual Ln_2O_3 in the recovered sample, and m_4 is the initial mass of UO_2 in each sample.

Subsequently, for the separation experiment of sample 3, a basket made of a denser molybdenum mesh was used to load the powder of UO_2 and La_2O_3 to prevent the UO_2 leakage. This time, the recovery efficiency of UO_2 was significantly elevated to 65.6%. Our results suggest that effective recovery of UO_2 can be achieved if an appropriate filter was used. Nevertheless, in our experiments, as Mo crucible and Mo basket were used, some UO_2 powder still leaked and floated on the surface of molten salt, which obviously decreases its recovery efficiency. For samples 2 and 3, the dissolution efficiency of UO_2 were 21 ± 1%, 8 ± 1% at 0.5 h, and 5 ± 1%, 7 ± 0.03% at 5 h, respectively.

In fact, we also tried to promote the separation by changing the amount of salt to reduce the volatilization of NH_4Cl, but found that if the amount of NH_4Cl is sufficient, the separation efficiency is not closely related to the amount of salt, which can be proved from the results of samples 1–3 (Fig. 4a–c).

Then the recovered products of samples 2 and 3 were characterized by XRD, as presented in Fig. 6. It is obvious that the recovered products of samples 2 and 3 only show the characteristic diffraction pattern of UO_2. It is worth mentioning that no diffraction peak of La_2O_3 was found in the samples before and after the separation, which should be due to the low content of La_2O_3.

Finally, the obtained UO_2 products were analyzed by ICP-AES to determine the content of residual Ln_2O_3. The removal efficiency of Ln_2O_3 was calculated according to the equation (6).

$$\eta_{remove} = \frac{m_1 - m_3}{m_1} \times 100\% \tag{6}$$

Where m_1 is the initial mass of Ln_2O_3, m_3 corresponds to the mass of residual Ln_2O_3 in the recovered samples.

The results showed that no residual La was detected in the recycled UO_2 products from sample 2 and sample 3, producing a removal efficiency of 100% for La_2O_3.

However, according to the La_2O_3 dissolution efficiency calculated from the La concentration in molten salt, it seems that La_2O_3 is not completely removed. This is due to the large error in the La (III) ion concentration obtained by ICP measurements. During ICP measurement, the salt sample is weighed in the air and easily adsorbs moisture, resulting in a concentration lower than the actual concentration. Therefore, we did not further calculate the separation factor based on the distribution of U and La in molten salt and recovered products.

3.3. Separation of UO_2 and La_2O_3 pellets

In order to prevent the diffusion of UO_2 into the molten salt, the mixed powder of UO_2 and La_2O_3 was further pressed into pellets and sintered at the temperature of 1473 K. The experimental conditions and results are displayed in Table 1 and Fig. 7. The contents of La_2O_3 in samples 4–6 were 1.0 wt%, 5.4 wt% and 10.8 wt%, respectively, and all the pellet samples were loaded in Mo crucible. It was found that the dissolution kinetics of La_2O_3 decreased after the powder was compressed into pellets. As shown in Fig. 7b and 7c, the concentration of soluble La^{3+} gradually increases within 5 h, indicating that the reaction proceeds if the amount of NH_4Cl is enough, which may be due to the fact that the reaction of La_2O_3 with NH_4Cl is diffusion controlled and depends on the diffusion of NH_4Cl from the pellet surface to the pellet bulk.

It is worth noting that the results of sample 4 differ from samples 5 and 6. As shown in Fig. 7a, the concentration of La ions does not change much and slightly decreases. This may be due to the low content of La_2O_3 in sample 4, in which the reaction of NH_4Cl with internal La_2O_3 is difficult to proceed, so that most of NH_4Cl is decomposed without chlorination effect. For samples 4–6, UO_2 is not found dissolved in LiCl–KCl molten salt from the ICP-AES determination. Further, the recovery efficiency of UO_2 in samples 4–6 (95.4%, 99.2%, and 81.6%, respectively) is greatly improved compared to that of powder samples, as shown in Table 1. In addition, the recovery efficiency of sample 6 was reduced compared to that of samples 4 and 5. The reasonable explanation is as follows: when the content of La_2O_3 in the pellet reaches 10.8 wt %, the mechanical strength of the pellet reduces much, and it breaks into several small pieces with powders during the separation process, as presented in Fig. 8c. In contrast, other pellets roughly remain intact during the recovery process (Fig. 8a and 8b), and the recovery efficiencies of these samples are relatively higher.

Unfortunately, despite the high UO_2 recovery efficiency, the removal efficiency of La_2O_3 was reduced. As displayed in Table 1, the removal efficiency of La_2O_3 in samples 4–6 is 63.1%, 82.0% and 57.0%, respectively. Compared to samples 1–3, the decrease in La_2O_3 removal efficiency in sample 4 is mainly due to the difficulty in reaction between NH_4Cl and La_2O_3 in the pellet bulk. On the other hand, as the content of La_2O_3 in the sample increases, the amount of NH_4Cl used for the reaction is not sufficient, resulting in

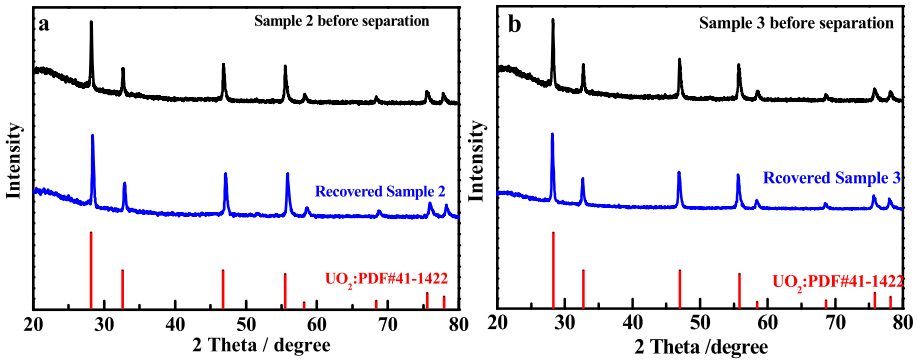

Fig. 6. The XRD results of (a) sample 2 and (b) sample 3.

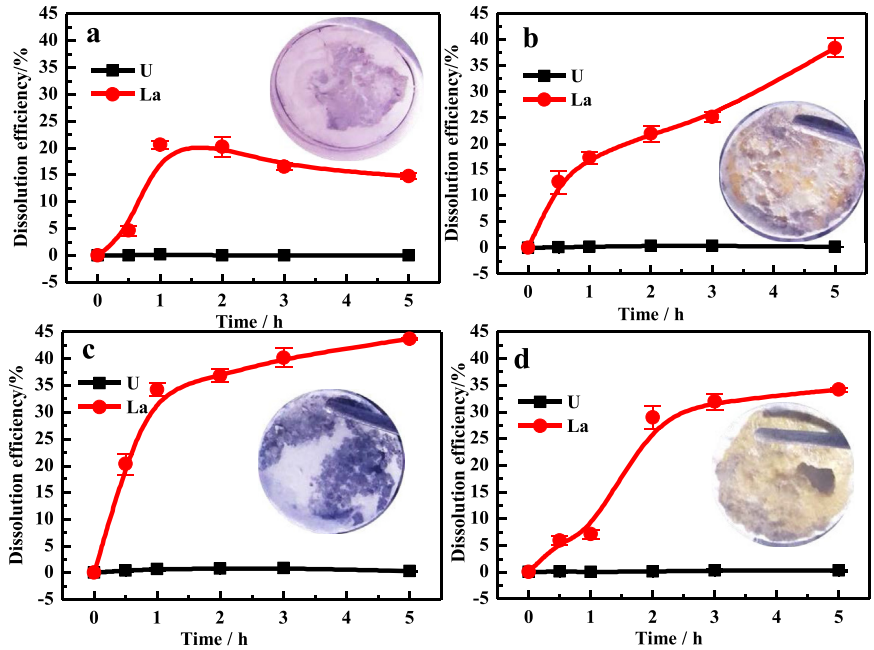

Fig. 7. Dissolution efficiency of UO_2 and La_2O_3 for pellet samples at 723 K: (a) sample 4, (b) sample 5, (c) sample 6, and (d) sample 7; the inset in each figure is the corresponding quenched salt of the sample after separation.

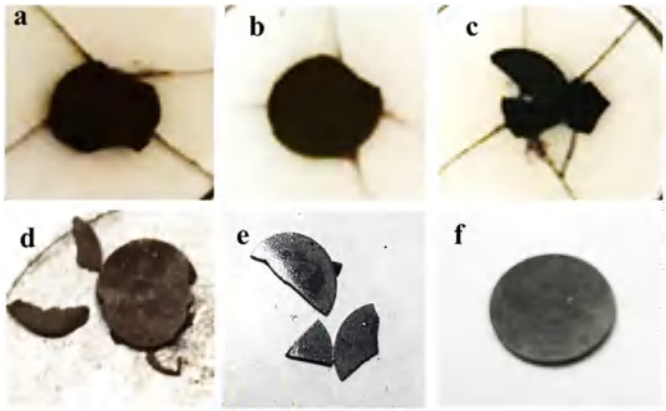

Fig. 8. The recovered pellets of (a) sample 4, (b) sample 5, (c) sample 6, (d) sample 7, (e) sample 8, and (f) sample 9.

the incomplete reaction of La_2O_3. Just as shown in Table 1, although the removal efficiency of La_2O_3 of sample 5 appeared to be higher than that of sample 4, the residual amount of La_2O_3 in the recovered product was 2.6 times that in sample 4. Further, when the content of La_2O_3 reached 10.8 wt% (sample 6), the residual amount of La_2O_3 was 4.7 times that of sample 5. These results indicate that the amount of NH_4Cl must be increased if higher removal efficiency of La_2O_3 is expected.

In the end, we selected the sample 7 with composition (1.0 wt% La_2O_3) close to the real spent fuel for verification. This time, the amount of NH_4Cl was increased to 3.5 g, and more LiCl–KCl quenched salt (76 g) was added to increase the depth of the salt for hindering the rapid volatilization of NH_4Cl. It can be seen from Fig. 7d that the concentration of La^{3+} ions in the molten salt gradually increases during the 5 h of dissolution. Finally, for sample 7, the recovery efficiency of UO_2 reached 92.0%, while the removal efficiency of La_2O_3 reached 94.4%. This shows that after a series of improvements, the separation method proposed in this paper is feasible.

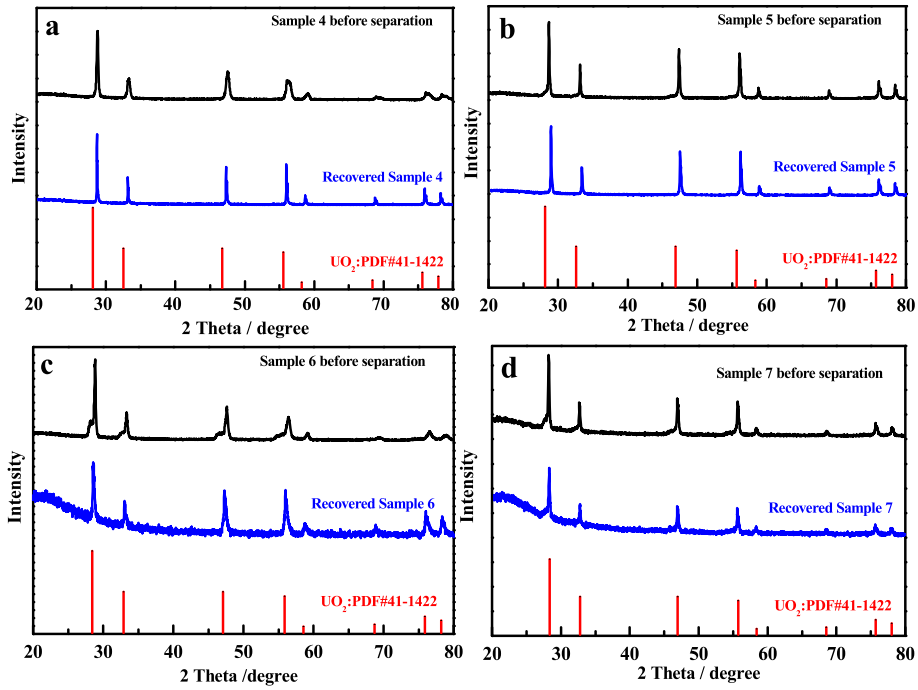

Fig. 9. The XRD results of (a) sample 4, (b) sample 5, (c) sample 6, and (d) sample 7.

Table 2
The experimental conditions and separation results of UO_2 and La_2O_3 at 723 K for the pellets sintered at 2023 K.

Sample No.	La_2O_3 content /wt%	m (UO_2+La_2O_3)/g	m_0 (LiCl−KCl)/g	m (NH_4Cl)/g	C_{La} in melt /wt%	m_2 (recovery sample)/g	m_3 (residual La_2O_3)/g	$\eta_{recovery}$ (UO_2)	η_{remove} (La_2O_3)
8	1.0	0.473	50	3.0	0.0002	0.459	0.0043	97.0%	8.5%
9	5.0	0.443	50	3.0	0.0003	0.440	0.0195	99.9%	11.9%

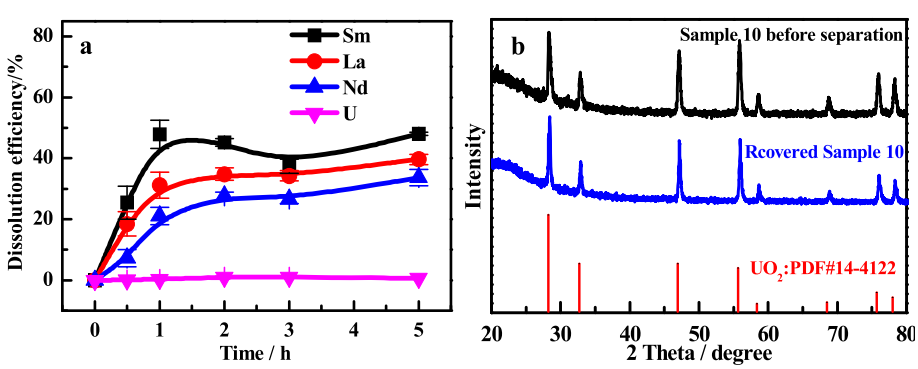

Fig. 10. (a) Dissolution efficiency of UO_2 and Ln_2O_3 for sample 10 at 723 K, and (b) the XRD result.

As shown in Fig. 9, due to the low content of La_2O_3, only diffraction peaks of UO_2 were observed in samples 4–7 before separation. Even though the amount of La_2O_3 in sample 6 had increased to 10.8 wt%, it is still small relative to the amount of UO_2. After the separation, the XRD results of the recovered product also showed only the diffraction peak of UO_2, which was almost the same as before the separation, which showed that no obvious crystal transformation occurred in UO_2 before and after the separation.

To further realistically simulate the uranium dioxide pellet nuclear fuel, we increased the sintering temperature of the pellets to 2023 K, with La_2O_3 content of 1.0 wt% (sample 8) and 5.0 wt% (sample 9). Obviously, as shown in Fig. 8 (e and f), the sample sintered at 2023 K is denser than that sintered at 1473K [33]. The high density of the pellets, which can reach 97% of the theoretical density [34,35], makes it difficult for the NH_4Cl to contact the La_2O_3 inside the pellets, resulting in poor separation. As shown in Table 2, La_2O_3 in sample 8 and 9 hardly reacted with NH_4Cl. The results show that for real fresh UO_2 fuel pellets, NH_4Cl is difficult to interact with Ln_2O_3 inside it. However, in the real pyroprocessing of UO_2 spent fuel, in order to remove the cladding, a voloxidation process is required to convert it into U_3O_8 powder [36]. U_3O_8 can be reduced to UO_2 again with Ar/H_2 mixed gas [37]. Therefore, this separation method still has a certain possibility.

Table 3
The experimental conditions and separation results of UO_2 and Ln_2O_3 for sample 10 at 723 K.

Ln_2O_3	Ln_2O_3 content /wt%	m (UO_2+Ln_2O_3)/g	m_0 (LiCl−KCl)/g	m (NH_4Cl)/g	C_U in melt /wt%	C_{Ln} in melt /wt%	m_2 (recovery sample)/g	m_3 (residual La_2O_3)/g	$\eta_{recovery}$ (UO_2)	η_{remove} (La_2O_3)
La_2O_3	1.2	0.694	80	3.5	0.0048	0.0034	0.638	0.0031	93.7%	61.7%
Sm_2O_3	1.1					0.0040		0.0038		52.0%
Nd_2O_3	1.1					0.0026		0.0033		55.2%

3.4. Separation of UO_2 and mixed Ln_2O_3

Further, we studied the separation of UO_2 and mixed lanthanide oxides (ie, sample 10). The sample was sintered at 1473 K, and the contents of La_2O_3, Nd_2O_3, and Sm_2O_3 were 1.2 wt%, 1.1 wt% and 1.1 wt %, respectively. As shown in Fig. 10, with the increase of dissolution time, the concentration of La and Nd in the molten salt gradually increased, and the concentration of Sm reached the highest value at 1 h and then fluctuated in a small range. The measured dissolution efficiency of La_2O_3, Sm_2O_3, and Nd_2O_3 was 39.7 ± 1.7%, 48.3 ± 0.5%, and 33.7 ± 2.9%, respectively, while UO_2 was insoluble. Subsequently, analysis of the recovered sample showed that the removal efficiency of La_2O_3, Sm_2O_3, and Nd_2O_3 was 61.7%, 52.0%, and 55.2%, respectively. The relatively low Ln_2O_3 removal efficiency is mainly due to the insufficient amount of NH_4Cl, because the Mo crucible used can only load a maximum of 3.5 g NH_4Cl. If the amount of NH_4Cl is increased, it can be predicted that the removal efficiency of Ln_2O_3 will be improved. Nevertheless, the recovery efficiency of UO_2 is as high as 93.7%, which proves that this method can also be used for the effective separation of UO_2 and mixed Ln_2O_3(see Table 3).

4. Conclusion

We propose a new method for separating UO_2 and lanthanide oxides without electrochemical techniques in LiCl−KCl molten salt, and La_2O_3 was used as a representative of lanthanide oxides to verify this method. Both powder and pellet samples were conducted. The La_2O_3 in the powder sample can be quickly dissolved in molten salt in 0.5 h, but some powder of UO_2 will react with trace amount of oxygen to form UO_2^{2+}, and the recovery efficiency of UO_2 powder is very low. For the pellet samples, the big advantage is that UO_2 after reaction can be readily recycled, but the removal of La_2O_3 becomes more difficult than powder samples. Finally, after optimization, the pellet sample can achieve high recovery efficiency and satisfactory La_2O_3 removal efficiency. Taken together, the pellet sample is more advantageous as it is less affected by residual oxygen in the glove box. Theoretically, if U_3O_8 is reduced to UO_2, this method is also expected to be applied to the separation of U_3O_8 and Ln_2O_3. In conclusion, this work can greatly simplify pyrochemical process without the electrochemical methods used, and it is promising to be further optimized and scaled up.

Declaration of competing interest

The authors declare that they have no known competing financial interests or personal relationships that could have appeared to influence the work reported in this paper.

CRediT authorship contribution statement

Yi-Chuan Liu: Investigation, Writing - original draft. **Ya-Lan Liu:** Conceptualization, Writing - review & editing, Project administration. **Yuan Zhao:** Formal analysis. **Zhe Liu:** Formal analysis. **Tong Zhou:** Formal analysis. **Qing Zou:** Formal analysis. **Xian Zeng:** Formal analysis. **Yu-Ke Zhong:** Validation. **Mei Li:** Visualization. **Zhong-xuan Sun:** Visualization. **Wei-Qun Shi:** Conceptualization, Resources, Supervision, Funding acquisition.

Acknowledgement

This work was supported by the Major Program of National Natural Science Foundation of China (No. 21790373), National Science Fund for Distinguished Young Scholars (No. 21925603).

Appendix A. Supplementary data

Supplementary data to this article can be found online at https://doi.org/10.1016/j.jnucmat.2020.152049.

References

[1] Y. Liu, K. Liu, L. Luo, L. Yuan, Z. Chai, W. Shi, Direct separation of uranium from lanthanides (La, Nd, Ce, Sm) in oxide mixture in LiCl-KCl eutectic melt, Electrochim. Acta 275 (2018) 100−109.
[2] J.-M. Gras, R.D. Quang, H. Masson, T. Lieven, C. Ferry, C. Poinssot, M. Debes, J.-M. Delbecq, Perspectives on the closed fuel cycle − implications for high-level waste matrices, J. Nucl. Mater. 362 (2−3) (2007) 383−394.
[3] K.-C. Song, H. Lee, J.-M. Hur, J.-G. Kim, D.-H. Ahn, Y.-Z. Cho, Status of pyroprocessing technology development in Korea, Nucl. Eng. Technol. 42 (2) (2010) 131−144.
[4] T. Inoue, L. Koch, Development of pyroprocessing and its future direction, Nucl. Eng. Technol. 40 (3) (2008) 183−190.
[5] H. Lee, J.-M. Hur, J.-G. Kim, D.-H. Ahn, Y.-Z. Cho, S.-W. Paek, Korean pyrochemical process R&D activities, Energy Procedia 7 (2011) 391−395.
[6] L.D. Brown, R. Abdulaziz, B. Tjaden, D. Inman, D.J.L. Brett, P.R. Shearing, Investigating microstructural evolution during the electroreduction of UO2 to U in LiCl-KCl eutectic using focused ion beam tomography, J. Nucl. Mater. 480 (2016) 355−361.
[7] W. Park, E.-Y. Choi, S.-W. Kim, S.-C. Jeon, Y.-H. Cho, J.-M. Hur, Electrolytic reduction of a simulated oxide spent fuel and the fates of representative elements in a Li 2 O-LiCl molten salt, J. Nucl. Mater. 477 (2016) 59−66.
[8] Y. Sakamura, T. Omori, Electrolytic reduction and electrorefining of uranium to develop pyrochemical reprocessing of oxide fuels, Nucl. Technol. 171 (3) (2017) 266−275.
[9] E.-Y. Choi, M.K. Jeon, J. Lee, S.-W. Kim, S.K. Lee, S.-J. Lee, D.H. Heo, H.W. Kang, S.-C. Jeon, J.-M. Hur, Reoxidation of uranium metal immersed in a Li 2 O-LiCl molten salt after electrolytic reduction of uranium oxide, J. Nucl. Mater. 485 (2017) 90−97.
[10] C.S. Seo, S.B. Park, B.H. Park, K.J. Jung, S.W. Park, S.H. Kim, Electrochemical study on the reduction mechanism of uranium oxide in a LiCl-Li2O molten salt, J. Nucl. Sci. Technol. 43 (5) (2006) 587−595.
[11] J.-M. Hur, S.M. Jeong, H. Lee, Underpotential deposition of Li in a molten LiCl−Li2O electrolyte for the electrochemical reduction of U from uranium oxides, Electrochem. Commun. 12 (5) (2010) 706−709.
[12] E.-Y. Choi, S.M. Jeong, Electrochemical processing of spent nuclear fuels: an overview of oxide reduction in pyroprocessing technology, Prog. Nat. Sci.: Mater. Int. 25 (6) (2015) 572−582.
[13] K. Liu, H.-B. Tang, J.-W. Pang, Y.-L. Liu, Y.-X. Feng, Z.-F. Chai, W.-Q. Shi, Electrochemical properties of uranium on the liquid gallium electrode in LiCl-KCl eutectic, J. Electrochem. Soc. 163 (9) (2016) D554−D561.
[14] P. Souček, L. Cassayre, R. Malmbeck, E. Mendes, R. Jardin, J.P. Glatz, Electrorefining of U-Pu-Zr-alloy fuel onto solid Aluminium cathodes in molten LiCl-KCl, Radiochim. Acta 96 (4−5) (2008).
[15] L.-X. Luo, Y.-L. Liu, N. Liu, L. Wang, L.-Y. Yuan, Z.-F. Chai, W.-Q. Shi, Electrochemical and thermodynamic properties of Nd (III)/Nd (0) couple at liquid Zn electrode in LiCl-KCl melt, Electrochim. Acta 191 (2016) 1026−1036.
[16] P. Masset, R.J.M. Konings, R. Malmbeck, J. Serp, J.-P. Glatz, Thermochemical properties of lanthanides (Ln=La,Nd) and actinides (An=U,Np,Pu,Am) in the molten LiCl−KCl eutectic, J. Nucl. Mater. 344 (1−3) (2005) 173−179.
[17] K. Fukasawa, A. Uehara, T. Nagai, N. Sato, T. Fujii, H. Yamana, Thermodynamic properties of trivalent lanthanide and actinide ions in molten mixtures of LiCl

and KCl, J. Nucl. Mater. 424 (1–3) (2012) 17–22.
[18] T. Yin, K. Liu, Y. Liu, Y. Yan, G. Wang, Z. Chai, W. Shi, Electrochemical and thermodynamic properties of uranium on the liquid bismuth electrode in LiCl-KCl eutectic, J. Electrochem. Soc. 165 (14) (2018) D722–D730.
[19] V. Smolenski, A. Novoselova, A. Osipenko, A. Maershin, Thermodynamics and separation factor of uranium from lanthanum in liquid eutectic gallium-indium alloy/molten salt system, Electrochim. Acta 145 (2014) 81–85.
[20] C.S. Wang, Y. Liu, H. He, F.X. Gao, L.S. Liu, S.W. Chang, J.H. Guo, L. Chang, R.X. Li, Y.G. Ouyang, Electrochemical separation of uranium and cerium in molten LiCl–KCl, J. Radioanal. Nucl. Chem. 298 (1) (2013) 581–586.
[21] N. Oecd, Physics and Safety of Transmutation Systems, A Status Report, 2006, p. 28.
[22] F.L. Fan, Z. Qin, S.W. Cao, C.M. Tan, Q.G. Huang, D.S. Chen, J.R. Wang, X.J. Yin, C. Xu, X.G. Feng, Highly efficient and selective dissolution separation of fission products by an ionic liquid [Hbet][Tf2N]: a new approach to spent nuclear fuel recycling, Inorg. Chem. 58 (1) (2019) 603–609.
[23] Y.-L. Liu, L.-X. Luo, N. Liu, B.-L. Yao, K. Liu, L.Y. Yuan, Z.-F. Chai, W.-Q. Shi, A particularly simple NH 4 Cl-based method for the dissolution of UO 2 and rare earth oxides in LiCl-KCl melt under air atmosphere, J. Nucl. Mater. 508 (2018) 63–73.
[24] S.E. Bae, T.S. Jung, Y.H. Cho, J.Y. Kim, K. Kwak, T.H. Park, Electrochemical formation of divalent samarium cation and its characteristics in LiCl-KCl melt, Inorg. Chem. 57 (14) (2018) 8299–8306.
[25] T. Hijikata, M. Sakata, H. Miyashiro, K. Kinoshita, T. Higashi, T. Tamai, Development of pyrometallurgical partitioning of actinides from high-level radioactive waste using a reductive extraction step, Nucl. Technol. 115 (1) (1996) 114–121.
[26] Y.-K. Zhong, K. Liu, Y.-L. Liu, Y.-X. Lu, T.-Q. Yin, L. Wang, Z.-f. Chai, W.-Q. Shi, Preparation of γ-uranium-molybdenum alloys by electrochemical reduction of solid oxides in LiCl molten salt, J. Electrochem. Soc. 166 (8) (2019) D276–D282.
[27] X. Ping, K. Liu, Y. Liu, L. Yuan, B. Yao, X. Zhao, Z. Chai, W. Shi, Direct electrochemical preparation of Ni-Zr alloy from mixture oxides in LiCl molten salt, J. Electrochem. Soc. 164 (13) (2017) D888–D894.
[28] T. Nagai, A. Uehara, T. Fujii, O. Shirai, N. Sato, H. Yamana, Redox equilibrium of U4+/U3+in molten NaCL-2CsCL by UV-vis spectrophotometry and cyclic voltammetry, J. Nucl. Sci. Technol. 42 (12) (2005) 1025–1031.
[29] V.A. Volkovich, I.B. Polovov, B.D. Vasin, T.R. Griffiths, C.A. Sharrad, I. May, J.M. Charnock, Effect of melt composition on the reaction of uranium dioxide with hydrogen chloride in molten alkali chlorides, Z. Naturforsch. 62 (10–11) (2007).
[30] Y.-H. Cho, S.-E. Bae, D.-H. Kim, T.-H. Park, J.-Y. Kim, K. Song, J.-W. Yeon, On the covalency of U(III)–Cl, U(IV)–Cl bonding in a LiCl–KCl eutectic melt at 450°C: spectroscopic evidences from their 5f–6d and 5f–5f electronic transitions, Microchem. J. 122 (2015) 33–38.
[31] T. Nagai, T. Fujii, O. Shirai, H. Yamana, Study on redox equilibrium of UO22+/U2+in molten NaCl-2CsCl by UV-vis spectrophotometry, J. Nucl. Sci. Technol. 41 (6) (2004) 690–695.
[32] T. Nagai, A. Uehara, T. Fujii, H. Yamana, Reduction behavior of in molten LiCl–RbCl and LiCl–KCl eutectics by using tungsten, J. Nucl. Mater. 439 (1–3) (2013) 1–6.
[33] R. Li, Y. Zhou, High temperature creep properties of UO2 fuel pellets manufactured by low temperature sintering technology, in: 2013 21st International Conference on Nuclear Engineering, American Society of Mechanical Engineers Digital Collection, 2013.
[34] J.H. Yang, K.W. Song, Y.W. Lee, J.H. Kim, K.W. Kang, K.S. Kim, Y.H. Jung, Microwave process for sintering of uranium dioxide, J. Nucl. Mater. 325 (2–3) (2004) 210–216.
[35] R. Singh, Isothermal grain-growth kinetics in sintered UO2 pellets, J. Nucl. Mater. 64 (1–2) (1977) 174–178.
[36] F. Gao, W.I. Ko, C.J. Park, S.K. Kim, H.H. Lee, Modeling and criticality evaluation of the voloxidation process, Ann. Nucl. Energy 38 (10) (2011) 2187–2194.
[37] E.-Y. Choi, J.W. Lee, J.J. Park, J.-M. Hur, J.-K. Kim, K.Y. Jung, S.M. Jeong, Electrochemical reduction behavior of a highly porous SIMFUEL particle in a LiCl molten salt, Chem. Eng. J. 207–208 (2012) 514–520.